EPJ manuscript No.
(will be inserted by the editor)

Generalized Blonder-Tinkham-Klapwijk theory and conductance spectra with particle-hole mixing interface potential

M. Catapano[1], F. Romeo[1,2], R. Citro[1,2], and F. Giubileo[1,2]

[1] Dipartimento di Fisica "E. R. Caianiello", Università degli Studi di Salerno, Via Giovanni Paolo II, I-84084 Fisciano (SA), Italy
[2] CNR-SPIN Salerno, Via Giovanni Paolo II, I-84084 Fisciano (SA), Italy

the date of receipt and acceptance should be inserted later

Abstract. We extend the Blonder-Tinkham-Klapwijk treatment including particle-hole mixing boundary conditions in the Bogoliubov-de Gennes scattering problem to describe anomalous conductance features often reported in normal-metal/superconductor junctions. We calculate the differential conductance spectra and show that conductance dips, not expected in the standard formulation, can be explained in terms of a phase π-shift between the bulk and the interface order parameter. A tight-binding model is also introduced to give a quantitative description of the phase-shift in terms of the transparency and polarization of the interface. We characterize the physics arising from particle-hole mixing boundary conditions at the interface and its effects on the conductance anomalies in superconductor-normal heterostructures.

PACS. 74.45.+c Proximity effects; Andreev reflection; SN and SNS ... – 74.25.-q Properties of superconductors

1 Introduction

Since the introduction of the point contact spectroscopy technique[1] in 70's, in which a micro-constriction is created pressing a metallic tip onto a superconducting sample, the study of normal-metal/superconductor (N/S) junctions has represented an important means for the comprehension of several physical phenomena at the interface. The BTK theory[2], formulated by Blonder-Tinkham - Klapwijk few years after, furnished a powerful tool to describe N/S contacts with transparency ranging from metallic to tunneling regime, the interface barrier strength being modeled using a Dirac delta potential of arbitrary amplitude. The theory, formulated in terms of Bogoliubov-de Gennes (BdG) equations[3], provides the transmission and reflection coefficients and it succeeds in explaining the conversion of a quasi-particle current into a supercurrent, due to the Andreev reflection[4], allowing accurate prediction of the experimental results about differential conductance spectra, energy gap and excess current. More recently, some modified BTK models have been proposed in order to take into account spin polarization[5–7], diffusive contacts[8–10], anisotropic superconducting order parameter [11–14], finite quasiparticle lifetime [15], superconducting proximity effect[7], external magnetic field [16] and thin ferromagnetic layers at the interface[17,18]. These formulations have been motivated by several experimental evidences[5,7,14,17–22] reporting unusual conductance features, namely conductance dips and anomalous values of the zero-bias conductance (ZBC), not expected in the standard BTK model.

From a mathematical point of view, including a Dirac delta potential within the BdG formalism, as done in the BTK approach, is equivalent to impose matching conditions for the scattering wavefunctions diagonal in the particle-hole representation[3]. However, off-diagonal boundary conditions in the Nambu space are also mathematically allowed and they could account for the appearance of anomalous features in the conductance spectra for N/S junctions.

In this paper we extend the BTK approach to include non-diagonal boundary conditions (in the particle-hole space) in the BdG scattering problem, by introducing an interface potential that mixes electron and hole components. We show that this potential describes the proximity effect at the interface and it is responsible for the formation of sub-gap conductance dips in the differential conductance spectra of N/S contacts. The comparison of the differential conductance curves with the experimental data suggests also that a phase π-shift between the bulk and the interface order parameter takes place, which could be due to a localized polarization at the interface. The latter hypothesis is carefully investigated by using a discretized model of the N/S junction.

The paper is organized as follows: in Sec. II we formulate the continuous model of the N/S interface introducing a particle-hole mixing term in the scattering potential. Off-diagonal boundary conditions are introduced and

the scattering coefficients are analytically determined. In Sec. III we show the differential conductance curves for N/S contacts obtained by using the generalized boundary conditions. We compare temperature evolution of conductance spectra with the existing theoretical models and available experimental data. Possible phase shift effects at the interface are discussed. In Sec. IV we use a discretized model to analyze the phase π-shift formation and discuss the necessary physical conditions to observe it. The physical meaning and the range of variability of the particle-hole mixing parameter Z_1 are discussed in Sec.V. Here we also report a comparison between the NS′S model and the generalized BTK model with particle-hole mixing potential. Conclusions are given in Sec. VI.

2 Model

We consider a one-dimensional N/S junction described by the BdG equations

$$\left[\mathcal{H}+V\left(x\right)\right]\psi\left(x\right)=E\psi\left(x\right), \tag{1}$$

which completely define the quasi-particle state $\psi\left(x\right)=\left(u_{\uparrow}\left(x\right),u_{\downarrow}\left(x\right),v_{\uparrow}\left(x\right),v_{\downarrow}\left(x\right)\right)^{t}$ having excitation energy E above the Fermi energy E_F. The Hamiltonian $\mathcal{H}$, which describes the bulk properties of the junction is

$$\mathcal{H}=\begin{pmatrix}\hat{H}_0 & \Delta(x)i\hat{\sigma}_y\\ -\Delta^*(x)i\hat{\sigma}_y & -\hat{H}_0^*\end{pmatrix}, \tag{2}$$

with

$$\hat{H}_0=\left[-\frac{\hbar^2\partial_x^2}{2m}-E_F\right]\hat{\mathbb{I}}, \tag{3}$$

where $\hat{\mathbb{I}}$ represents the identity operator in the spin space and $\hat{\sigma}_y$ is the Pauli matrix. We assume that the Fermi energy E_F and the effective mass m in the normal side of the junction ($x<0$) are equal to those in the superconductor ($x>0$), while the superconducting order parameter is taken of the form $\Delta(x)=\Delta\theta(x)$, where $\theta(x)$ is the Heaviside step function. Differently from the standard BTK treatment, we model the potential barrier at the interface ($x=0$) by a particle-hole mixing operator

$$V\left(x\right)=\begin{pmatrix}U_0\hat{\mathbb{I}} & iU_1\hat{\sigma}_y e^{i\varphi}\\ -iU_1\hat{\sigma}_y e^{-i\varphi} & -U_0\hat{\mathbb{I}}\end{pmatrix}\delta\left(x\right), \tag{4}$$

where U_0 indicates the usual BTK barrier strength, while the term U_1 describes the interfacial electron-hole coupling strength. The off-diagonal components of $V(x)$ describe the presence of a weak superconducting interface[23] which can be intuitively understood in terms of proximity effect. The variable φ represents the phase difference between the interface and the bulk superconducting order parameter. Maintaining arbitrary values of φ, a Josephson current $I_J(\varphi)\propto\sin(\varphi)$[24] is expected to flow through the interface. The free energy of the system is expected to be minimized when Josephson current vanishes, i.e. for $\varphi=0$ or π, the value $\varphi=0$ being a free energy minimum of the N/S junction. On the other hand, the value $\varphi=\pi$ can become an energy minimum if a local polarization is formed at the interface (e.g., transition metals easily oxidize producing localized magnetic states[25,26]). Indeed, in the presence of a sufficiently strong magnetic moment, the interfacial phase can be modified from 0 to π and the sign change of the interfacial order parameter follows a mechanism similar to the one described in Ref.[27].

In the following, we calculate the differential conductance of the N/S junction by considering the generalized boundary conditions of the scattering problem. The wave function of an electron with spin $\sigma=\{\uparrow,\downarrow\}$ coming from the N-side of the junction is given by:

$$\begin{aligned}\psi_N^{\sigma}(x)=&\begin{pmatrix}\delta_{\uparrow\sigma}\\ \delta_{\downarrow\sigma}\\ 0\\ 0\end{pmatrix}e^{ikx}+r_e^{\uparrow}\begin{pmatrix}1\\0\\0\\0\end{pmatrix}e^{-ikx}\\ &+r_e^{\downarrow}\begin{pmatrix}0\\1\\0\\0\end{pmatrix}e^{-ikx}+r_h^{\uparrow}\begin{pmatrix}0\\0\\1\\0\end{pmatrix}e^{iqx}\\ &+r_h^{\downarrow}\begin{pmatrix}0\\0\\0\\1\end{pmatrix}e^{iqx}.\end{aligned} \tag{5}$$

Here the coefficients $r_e^{\uparrow,\downarrow}$ and $r_h^{\uparrow,\downarrow}$ correspond, respectively, to normal reflection and Andreev reflection, while $\hbar k=\sqrt{2m\left(E_F+E\right)}$ and $\hbar q=\sqrt{2m\left(E_F-E\right)}$ indicate the electron and hole wave vectors.
In the superconducting region, we have

$$\begin{aligned}\psi_S(x)=&t_e^{\uparrow}\begin{pmatrix}u\\0\\0\\v\end{pmatrix}e^{ik_+x}+t_e^{\downarrow}\begin{pmatrix}0\\u\\-v\\0\end{pmatrix}e^{ik_+x}\\ &+t_h^{\downarrow}\begin{pmatrix}v\\0\\0\\u\end{pmatrix}e^{-ik_-x}+t_h^{\uparrow}\begin{pmatrix}0\\v\\-u\\0\end{pmatrix}e^{-ik_-x},\end{aligned} \tag{6}$$

where the coefficients $t_e^{\uparrow}$, $t_e^{\downarrow}$, $t_h^{\uparrow}$, $t_h^{\downarrow}$ correspond to the transmission as electron-like and hole-like quasiparticle with wave vectors $\hbar k_{\pm}=\sqrt{2m\left(E_F\pm\sqrt{E^2-\Delta^2}\right)}$, the BCS[28] coherence factors being

$$u^2=1-v^2=\frac{1}{2}\left(1+\frac{\sqrt{E^2-\Delta^2}}{E}\right). \tag{7}$$

The coefficients in Eqs. (5) and (6) can be determined by using the generalized boundary conditions for the wave functions at the interface:

$$\begin{aligned}\psi_N^{\sigma}(0)&=\psi_S(0)\\ \partial_x\psi_S|_{x=0}-\partial_x\psi_N^{\sigma}|_{x=0}&=\mathcal{A}\,\psi_S(0).\end{aligned} \tag{8}$$

The matching matrix

$$\mathcal{A}=k_F Z_0\hat{\mathbb{I}}_{4\times4}+k_F Z_1\begin{pmatrix}0 & i\hat{\sigma}_y e^{i\varphi}\\ i\hat{\sigma}_y e^{-i\varphi} & 0\end{pmatrix} \tag{9}$$

contains a diagonal term in the particle-hole representation with the usual BTK parameter $Z_0 = 2mU_0/(\hbar^2 k_F)$, and off-diagonal terms of strength $Z_1 = 2mU_1/(\hbar^2 k_F)$, where the meaning and the variability range of the parameter Z_1 are discussed in Sec. V. The Eqs. (8)-(9) provide the simplest particle-hole mixing boundary conditions mathematically allowed by the BdG formulation.
Using the above boundary conditions on the wave functions and the Andreev approximation ($k_+ = k_- = k = q = k_F$), we find the following expression for the scattering coefficients assuming the injection of a spin-up electron from the normal side (the result doesn't depend on the spin of the incoming process)

$$
\begin{aligned}
r_h^{\downarrow} &= \frac{4uv - 2ie^{-i\varphi}Z_1(u^2-v^2)}{4u^2 + 4iuvZ_1\cos\varphi + (u^2-v^2)(Z_0^2+Z_1^2)} \qquad (10)\\
r_e^{\uparrow} &= -\frac{4iuvZ_1\cos\varphi + (u^2-v^2)[Z_0(2i+Z_0)+Z_1^2)]}{4u^2 + 4iuvZ_1\cos\varphi + (u^2-v^2)(Z_0^2+Z_1^2)}\\
t_e^{\uparrow} &= \frac{4u - 2i(uZ_0 - vZ_1e^{-i\varphi})}{4u^2 + 4iuvZ_1\cos\varphi + (u^2-v^2)(Z_0^2+Z_1^2)}\\
t_h^{\downarrow} &= \frac{2i(vZ_0 - uZ_1e^{-i\varphi})}{4u^2 + 4iuvZ_1\cos\varphi + (u^2-v^2)(Z_0^2+Z_1^2)},
\end{aligned}
$$

while the absence of spin-flip scattering implies $r_e^{\downarrow} = r_h^{\uparrow} = t_e^{\downarrow} = t_h^{\uparrow} = 0$. Once the scattering coefficients are obtained, we can calculate the differential conductance by the formula [2]

$$
G(V) \propto \sum_{\sigma} \int dE\,[1 + A_{\bar{\sigma}} - B_{\sigma}] \left[-\frac{\partial f(E-eV)}{\partial E}\right] \qquad (11)
$$

where $A_\sigma = |r_h^\sigma|^2$ and $B_\sigma = |r_e^\sigma|^2$ are the Andreev reflection and normal reflection probabilities, respectively, $f(E)$ is the Fermi-Dirac distribution, while the notation $\bar{\sigma}$ indicates the spin polarization opposite to σ.

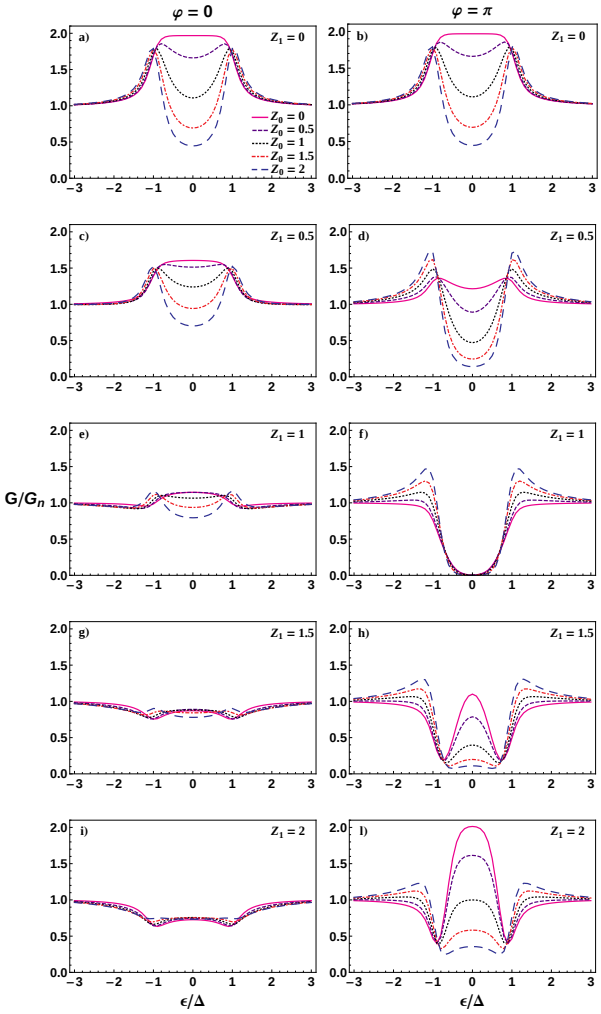

Fig. 1. (Color online) Normalized differential conductance curves, G/G_n *vs* ϵ/Δ, calculated at $T = 1.6K$ from Equation (11). The different curves are obtained for distinct values of Z_0, Z_1 and φ (values in the panels).

3 Results

We first study the finite temperature conductance spectra of the N/S junction emphasizing the effects of the barrier strengths Z_0, Z_1 and of the phase φ. In Figure 1 we show the normalized conductance G/G_n *vs* ϵ/Δ, with $G_n = G(eV \gg \Delta)$, for different values of Z_0 and Z_1 at a fixed temperature $T = 1.6K$, computed by using Eq. (11). Two cases are considered: (i) $\varphi = 0$, shown in the left panels; (ii) $\varphi = \pi$, shown in the right panels. In each plot, different curves correspond to different Z_0 values (ranging from 0 to 2), while Z_1 is fixed as labelled.
For $\varphi = 0$ and $Z_1 = 0$ (Figure 1(a)) the usual BTK behavior is recovered. In this case, the zero-bias conductance is suppressed as Z_0 is increased, while two peaks at $\epsilon/\Delta \approx \pm 1$ appear. Fixing $Z_1 = 0.5$ (Fig. 1(c)), we observe a reduction of the amplitude of the zero bias conductance feature compared to the $Z_1 = 0$ case. The difference between the conductance lowering induced by Z_0 and the peculiar amplitude reduction induced by Z_1 is evident: while the increasing of Z_0 induces a zero-bias conductance minimum, a tendency to increase the zero-bias conductance is observed by rising Z_1 to 1.0 (Fig. 1(e)), $Z_1 = 1.5$ (Fig. 1(g)) and $Z_1 = 2$ (Fig. 1(i)).
A different scenario is observed for $\varphi = \pi$: the effect of moderate values of Z_1, namely $Z_1 = 0.5$ (Fig. 1(d)) and $Z_1 = 1$ (Fig. 1(f)), combines with Z_0 to give a relevant effective barrier strength leading to a strong suppression of the sub-gap conductance up to fully gapped spectra. For $Z_1 = 1.5$ (Fig. 1(h)) and $Z_1 = 2$ (Fig. 1(l)) an evident zero-bias peak with two dips at $\epsilon/\Delta \approx \pm 1$ appears. Such ZBC peak exists for all Z_0 values in the range $[0, 2]$, the junction transparency reduction having effect only on the peak amplitude.
All the conductance structures presented above (coming from the generalized boundary conditions) cannot be recovered within the standard BTK approach (except for the case Z_1=0). Moreover, the interface potential given in Equation (4) can be further generalized to include, spin-orbit interaction in the plane perpendicular to the trans-

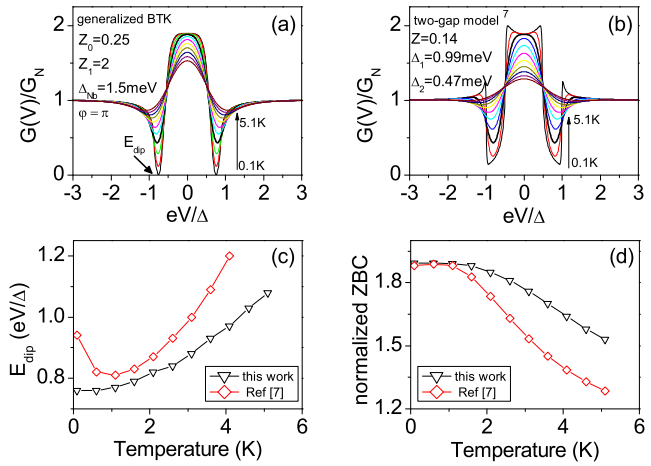

Fig. 2. Temperature evolution of the normalized conductance curves obtained for (a) generalized BTK model with particle-hole mixing boundary conditions and for (b) two-gap model[7] for the parameters Z=0.14, Δ_1=0.99 meV (bulk gap), Δ_2=0.47 meV (proximized gap). The thick black line in the two plots represent the best fit for Cu/Nb experimental data reported in Ref.[7]. (c) Comparison of the temperature evolution of the energy position of the conductance dips, E_{dip} vs T, obtained from (a) and (b). (d) Comparison of the temperature evolution of the ZBC, obtained from (a) and (b).

port direction, local magnetic moments and triplet or non-centrosymmetric superconducting correlations. The above complications make the interface potential an off-diagonal differential operator of the form $\mathcal{B}(x, \partial_{x,y,z})\delta(x)$ acting on the Nambu space which induces an extended class of particle-hole mixing boundary conditions. Extending the BTK theory along this direction produces analytic results for the scattering coefficients which can be directly employed to explain anomalous conductance spectra.

In Figure 2 we compare the temperature evolution of the conductance spectra obtained in the generalized BTK model introduced above, with the one calculated by using the transmission and reflection coefficients of the two-gap model of Ref. [7] characterized by the barrier height Z and two gap values at the interface Δ_1 and Δ_2. Both models can be used to reproduce (black solid lines in Fig. 2(a) and 2(b)) the experimental data reported for Cu/Nb contacts in Ref.[7]. In particular, in Fig. 2(a) we show theoretical curves calculated in the temperature range between 0.1 K and 5.1 K by assuming Z_0=0.35, Z_1=2, Δ_{Nb}=1.5 meV, $\varphi = \pi$, while in Fig. 2(b) the conductance curves are obtained by considering the parameters Z=0.14, Δ_1=0.99 meV, Δ_2=0.47 meV, in the two-gap model. Let us note that the value $\varphi = \pi$ represents the best fitting parameter to reproduce the experimental findings of subgap dips in the N/S junction under discussion. For both the theoretical curves the temperature is fixed at the value $0.9K$ that is lower than the bath temperature due to non-equilibrium effects [7] or other physical effects [18]. The temperature evolution of the conductance spectra within the two models shows a different behavior of the ZBC and E_{dip}. By rising the temperature, a non-monotonic evolution of E_{dip}

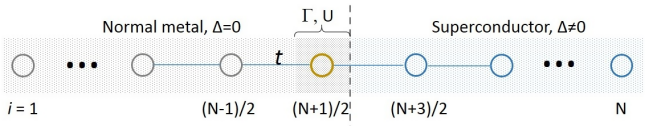

Fig. 3. Discretized model of the N/S junction consisting of N (odd) sites: (N+1)/2 normal sites ($\Delta = 0$) and (N-1)/2 superconducting sites ($\Delta \neq 0$); magnetic (Γ) e non-magnetic (U) potentials are present at the interface site $i = (N+1)/2$. The hopping parameter t is homogeneous along the system.

(Fig. 2(c)) and a faster reduction of ZBC (Fig. 2(d)) is observed for the case of Fig. 2(b). As a consequence, very low temperature experiments are necessary to distinguish the two models and for understanding the physical origin of the anomalous conductance features observed in the point contact experiments in N/S devices. It is worth noticing that both models are physically plausible. Indeed, Nb and Cu oxides are known to exhibit magnetic correlations that could realize effective local polarization enabling a phase shift of π at the interface; on the other hand, the formation of a (proximized) weak superconducting layer at the N/S interface (two-gap model) is also possible.

4 Discretized model

As we have seen in Figs. 1 and 2 the conductance dips appear in the generalized BTK approach for $\varphi = \pi$ and this phase value can be associated to a localized polarization at the interface. In fact, its presence can make a phase gradient of π energetically favorable. In order to identify the physical conditions (interface polarization and transparency) to realize the π-shift, we consider a discretized formulation that allows to describe spatial dependent potentials without increasing the computational complexity. We model a system with an odd number of sites N in which $(N-1)/2$ sites are used for both the normal and the superconducting side, while one normal site with magnetic (Γ) and non-magnetic potential (U) is considered at the interface (see Fig. 4). The nearest-neighbor hopping parameter $t = \hbar^2/(2ma^2)$, expressed in terms of the sites distance a, is assumed homogeneous and it is used as energy unit, $t \simeq 10 \cdot \Delta_{Nb}$ in order to have $\xi_{Nb} \simeq 10 \cdot a$. Temperature is measured in dimensionless units $\tau = k_B T/t$. Hereafter, we set $t = 16.2$ meV as the energy cut-off of the theory, the latter being of the same order of magnitude of the Debye energy $\hbar\Omega_D$. This choice guarantees that only states with phonon-mediated attraction (i.e. with $\epsilon \in [0, \hbar\Omega_D]$) are retained. Under these assumptions, the relevant wave functions present a De Broglie wavelength greater than the lattice constant a, while the associated eigenvalues have a near-parabolic energy dispersion.

The discretized version of the BdG equations with a Zeeman term $\Gamma(x)\hat{\sigma}_z$ added to the single-particle Hamiltonian $\hat{H}_0$ to account for the effective polarization at the interface corresponds to the following matrix equations

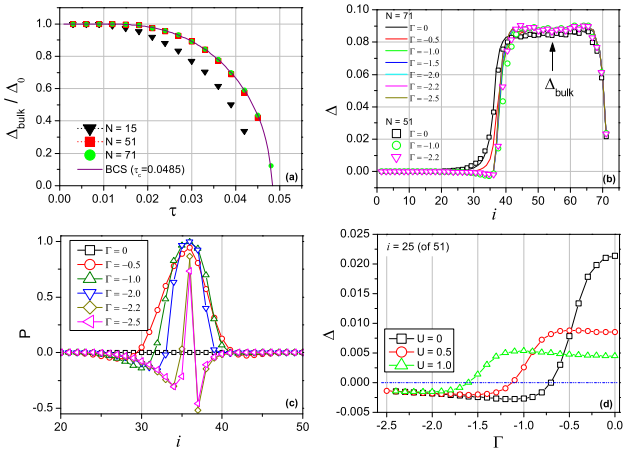

Fig. 4. Numerical results obtained in the discretized model. (a) Temperature dependence of the bulk superconducting gap for different systems, namely $N = 15$, $N = 51$, $N = 71$, assuming transparent barrier, $U = 0$. Numerical data, normalized to the low temperature value Δ_0, are compared to theoretical behaviour expected in the BCS model for $\tau_c = 0.0485$. (b) Spatial dependence of the superconducting gap for 71-sites and 51-sites systems, by assuming $U = 0$, a constant BCS coupling, $\lambda_i = \lambda$, and dimensionless temperature $\tau = 0.025$. Different curves correspond to different values of Γ. Lines refer to data obtained for 71-sites system; scattered symbols refer to 51-sites system, rescaled to compare the data sets. The arrow indicates the region where the superconducting gap is calculated self-consistently. (c) Spatial dependence of the polarization calculated for $N = 71$ for different Γ values, with $U = 0$ and $\tau = 0.025$. (d) Effect of the barrier strength U: the superconducting gap vs Γ is evaluated at the site $i = 25$ (of 51), at $\tau = 0.025$ for three different transparency conditions ($U = 0$, $U = 0.5$, $U = 1$), the magnetic site being located at $i = 26$.

$(\forall\ i \in [1, N])$:

$$\mathcal{M}_i^{(\sigma)} \Psi_i^{(\sigma)} + T\left(\Psi_{i+1}^{(\sigma)} + \Psi_{i-1}^{(\sigma)}\right) = 0, \tag{12}$$

where $(\sigma = \pm,\ \pm \equiv \uparrow / \downarrow)$

$$\mathcal{M}_i^{(\sigma)} = \begin{pmatrix} \varepsilon_i - E + \sigma\Gamma_i & \sigma\Delta_i \\ \sigma\Delta_i^* & -\varepsilon_i - E + \sigma\Gamma_i \end{pmatrix}, \tag{13}$$

while $T = -t\,\hat{\sigma}_z$. Here $\varepsilon_i/t = 2 + U\delta_{i,(N+1)/2}$ is the energy of the i-th lattice site[29], while $\Psi_i^{(\sigma)} = (u_{\sigma,i}, v_{\bar{\sigma},i})^t$ is the discretized BdG state in the absence of spin-flip scattering. $\Gamma_i/t = \Gamma\delta_{i,(N+1)/2}$ is the site dependent Zeeman energy that we take different from zero only at the interface site. Using Dirichlet boundary conditions $\Psi_1^{(\sigma)} = \Psi_N^{(\sigma)} = 0$, we get electron-like eigenstates

$$\Phi^{(\sigma,n)} = \sum_{i=1}^{N} \mathcal{A}_i \otimes \left(u_{\sigma,i}^{(n)}, v_{\bar{\sigma},i}^{(n)}\right)^t \tag{14}$$

associated to positive energy eigenvalues ($\epsilon_n \geq 0$), with $\mathcal{A}_i = (\delta_{1,i}, ..., \delta_{N,i})^t$. The spatial dependence of the superconducting gap is computed as[30]

$$\Delta_i = \frac{\lambda_i}{2} \sum_n \left[u_{\uparrow,i}^{(n)} v_{\downarrow,i}^{(n)\star} - u_{\downarrow,i}^{(n)} v_{\uparrow,i}^{(n)\star}\right] \tanh\left(\frac{\epsilon_n}{2k_B T}\right), \tag{15}$$

the sum being calculated for $\epsilon_n \in [0, \hbar\Omega_D]$. The attractive phonon-mediated local potential λ_i is assumed constant[31] ($\lambda_i = \lambda$) also in the normal side of the junction to take into account proximity effects. We consider the bulk superconducting gap Δ_{bulk} at the center of the S-region, in order to avoid finite size effects. Δ_{bulk} is computed self-consistently using Eq. (15) with an accuracy greater than 1% starting from $\Delta_i = 0.15t$ in S, and by fixing $\lambda = 2.4\ t$. The polarizing effect of the magnetic site at the interface can be quantified by the site-dependent polarization $P_i = (n_{i,\uparrow} - n_{i,\downarrow})/(n_{i,\uparrow} + n_{i,\downarrow})$, where

$$n_{i,\uparrow} + n_{i,\downarrow} = \sum_n \left[|u_{\uparrow,i}^{(n)}|^2 f_n + |v_{\downarrow,i}^{(n)}|^2 (1 - f_n)\right] + \tag{16}$$
$$+ \sum_n \left[|u_{\downarrow,i}^{(n)}|^2 f_n + |v_{\uparrow,i}^{(n)}|^2 (1 - f_n)\right]$$

and

$$n_{i,\uparrow} - n_{i,\downarrow} = \sum_n \left[|u_{\uparrow,i}^{(n)}|^2 f_n - |v_{\downarrow,i}^{(n)}|^2 (1 - f_n)\right] + \tag{17}$$
$$+ \sum_n \left[-|u_{\downarrow,i}^{(n)}|^2 f_n + |v_{\uparrow,i}^{(n)}|^2 (1 - f_n)\right],$$

with $f_n = f(\epsilon_n)$ a shortened notation standing for the Fermi-Dirac distribution. In order to capture the bulk-like behaviour using a finite size system, the system size N has been progressively increased from $N = 15$ to $N = 71$, while monitoring the temperature dependence of Δ_{bulk}. The results of this analysis are shown in Figure 5(a) where normalized values of Δ_{bulk} are presented as a function of the dimensionless temperature τ. For a system size of $N = 15$ a size-induced suppression of the superconducting gap is observed, this effect being more evident close to the transition temperature τ_c. Increasing the system size up to $N = 51$ produces a Δ_{bulk} vs τ curve very close to the one obtained for the $N = 71$ case, signaling that the bulk limit of the interface model has been reached. The temperature evolution of Δ_{bulk} for $N = 71$ has been compared with the BCS behaviour giving a dimensionless critical temperature $\tau_c = 0.0485$, corresponding to a niobium critical temperature $T_c^{Nb} \simeq 9.1K$. In Figure 5(b) we present the spatial dependence of the superconducting gap (for system size $N = 51$ and $N = 71$) fixing the Zeeman energy Γ of the magnetic potential in the range $[-2.5, 0]$, while taking $U = 0$ (transparent interface) and $\tau = 0.025$ (i.e. $T \sim T_c^{Nb}/2$). In order to compare spectra obtained for systems with different size, the data referring to $N = 51$ have been rescaled. For $-1.0 < \Gamma < 0$ we observe ordinary proximity effect where finite superconducting order parameter is induced in the N-side on a length of about $10a \simeq \xi_{Nb}$. For sufficiently strong magnetization $\Gamma \leq -1.0$ negative order parameter is induced on the same length

scale. Reduction of the order parameter on the right border is due to the S/vacuum interface. In Figure 5(c) we show the spatial dependence of the polarization, calculated for $\Gamma \in [-2.5, 0]$ and $U = 0$. The polarizing effect of the localized magnetic moment asymmetrically extends on a distance of about $20a$. In the superconducting side the induced polarization is inverted for large Γ values[32] ($\Gamma < -2.0$). The general aspect of the polarization curves evidences Friedel density oscillations. We have also verified the effect of barrier strength on the inversion of the superconducting order parameter. In Figure 5(d), we show the gap value calculated (at site $i = 25$) in proximity of the interface, for a system size $N = 51$, as a function of Γ, with enhanced resolution (step 0.1). For reduced transparency ($U > 0$) a larger magnetic moment is necessary to induce the inversion of the interface order parameter. The analysis of the pairing potential Δ_i shows that, in presence of a local polarization at the interface, a phase gradient $\varphi = \pi$ can be stabilized. For relatively transparent junctions (i.e. described by small values of U) the sign change of the interface order parameter can be obtained with moderate polarization strength, while strong polarization values are needed for opaque interface with higher values of U. Thus the probability to observe an hidden magnetic moment at the interface accompanied by a phase gradient is enhanced in transparent systems. The physical origin of a local magnetic moment at the Cu/Nb interface probably resides in many-body effects which can be accounted for in the framework of the Anderson impurity model[26].

5 Discussion

In this Section we discuss the range of variability of the particle-hole mixing parameter Z_1 that we have added to the standard BTK theory and the validity of the generalized BTK model.
As we have seen in Eq.(4), the off-diagonal potential mimicking the superconducting proximity effect is given by:

$$V^{eh}(x) = \begin{pmatrix} 0 & i\hat{\sigma}_y e^{i\varphi} \\ -i\hat{\sigma}_y e^{-i\varphi} & 0 \end{pmatrix} U_1 \delta(x). \qquad (18)$$

Hereafter, we would like to connect the phenomenological parameter U_1 to the microscopic parameters of the junction. Requiring that the spatial average of $V^{eh}(x)$ over the proximized normal region, i.e. $x \in [-\xi, 0^+]$, is related to the average pairing $|\bar{\Delta}|$ experienced by the particles at the interface, we get the equation:

$$\xi^{-1} \int_{-\xi}^{0^+} V^{eh}(x)\, dx = |\bar{\Delta}| \begin{pmatrix} 0 & i\hat{\sigma}_y e^{i\varphi} \\ -i\hat{\sigma}_y e^{-i\varphi} & 0 \end{pmatrix}. \qquad (19)$$

Solving Equation (19), we obtain $U_1 = \xi|\bar{\Delta}|$, with $|\bar{\Delta}| > 0$. From the above argument we can write $Z_1 = \frac{2m\xi|\bar{\Delta}|}{\hbar^2 k_F} = \frac{|\bar{\Delta}|k_F\xi}{E_F}$. Moreover, recalling the expression of the coherence length $\xi \approx \hbar v_F/(2\Delta_{bulk})$, the mixing strength Z_1 can be represented in the form of ratio $Z_1 = |\bar{\Delta}|/\Delta_{bulk}$. Assuming that $|\bar{\Delta}|$ is just a fraction of the bulk pairing potential Δ_{bulk}, one expects small mixing strength. However its value is increased in the presence of band bending effects due to charge transfers and orbital reconstruction which can significantly modify the quasi-particle effective mass m, the Fermi energy E_F and the particles velocity v_F at the interface.
E.g. for a niobium-based interface characterized by $k_F\xi \approx 400$ ($\xi_{Nb} \approx 40$ nm, $k_{F,Nb}^{-1} \sim 0.1$ nm) and $|\bar{\Delta}| \approx 0.5$ meV ($0.3\Delta_{bulk}$), using $Z_1 = \frac{|\bar{\Delta}|k_F\xi}{E_F}$, we get $Z_1 = 0.2/E_F$, the Fermi energy being measured in eV. Since in nanostructured systems (thin films) E_F can take values significantly lower than 1 eV, we can conclude that Z_1 can be of the order and greater than 1 (e.g. $Z_1 \simeq 1.3$ for $E_F = 0.15$ eV). Values of $Z_1 \simeq 2$ can be reached considering $|\bar{\Delta}| \approx 0.5\Delta_{bulk}$ and $E_F = 0.15$ eV. This simple argument justifies the values of Z_1 greater than unity used in Fig.2.

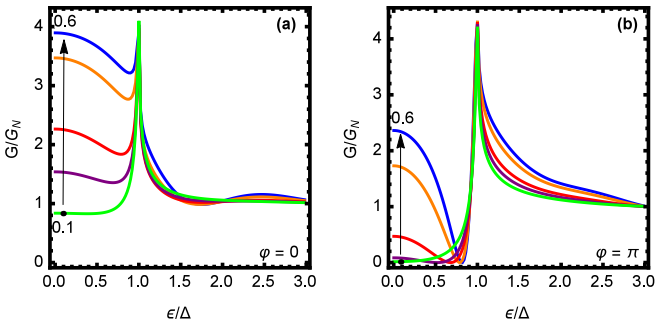

Fig. 5. Zero temperature conductance curves obtained in the NS′S model as a function of ϵ/Δ. Different curves in both panels are obtained fixing the ratio $\Delta'/\Delta_{bulk} = 0.1$ (lowest curve), 0.2, 0.3, 0.5, 0.6 (highest curve). The remaining parameters are $Z = 2.5$, $k_F d = 380$ and $\varphi = 0$ (left panel) or $\varphi = \pi$ (right panel).

However a better insight on the role of Z_1 can be inferred by studying the conductance in a NS′S model, where S is the bulk superconductor and S′ is the superconducting proximity region of length $d \sim \xi$ with a gap modulus $\Delta' < \Delta_{bulk}$. The N/S′ interface is assumed to be transparent, while the opacity of S′/S interface is controlled by the barrier strength Z. Calculating the Andreev and normal reflection coefficients by using the usual BTK boundary condition of the scattering wavefunction at the N/S′ interface and S′/S interface, we can evaluate the zero temperature differential conductance for a phase difference between S and S′, $\varphi = 0$ or π. The results are reported in Fig.5 where the zero temperature conductance G/G_N is plotted as a function of ϵ/Δ. The different curves are obtained at varying the ratio Δ'/Δ_{bulk} (0.1 to 0.6 from below), while fixing the remaining parameters as $Z = 2.5$, $k_F d = 380$ (of the order of the coherence length $k_F\xi = 400$) and $\varphi = 0$ (left panel) or $\varphi = \pi$ (right panel). Here it is shown that zero conductance dips within the gap are obtained for $\varphi = \pi$ and an high value of Z (right panel of Fig.5). This indicates that the role of Z_1 in the generalized BTK model is similar to that of the ratio Δ'/Δ_{bulk} in

the NS′S model under the assumption of low-transparency of the S′/S interface. This is confirmed observing that the dip-peak structure in Fig.1 (right column) appears as Z_1 is increased ($Z_1 > 1$). The same effect is obtained in the NS′S model by increasing Δ'/Δ_{bulk} in the presence of low-transparency of the barrier (high value of Z). This suggests that the parameter Z_1 not only retains information on the proximity effect but also contributes to renormalize the interface transparency producing a more opaque local potential. The comparison between the generalized BTK model and the NS′S model shows that the dip-peak structure in the conductance is not an artifact of the delta-like form of the particle-hole mixing potential but it is related to a genuine proximity effect, which can also be studied in the framework of an NS′S model setting high Z values (tunnel limit) and moderate Δ'/Δ_{bulk} ratio. Let us finally note that the NS′S model we have considered here, differs from the two-gap model of Ref.[7] where the results for the conductance do not depend on the proximity region length d and on the relative superconducting phase φ.

6 Conclusions

We have generalized the BTK theory to include particle-hole mixing boundary conditions in the scattering problem, reporting analytic results for the scattering coefficients. The extended theory allows a complete parametrization of the interface effects in terms of three parameters, namely Z_0, Z_1 and φ. We calculated the finite-temperature differential conductance spectra for N/S junctions showing the formation of conductance dips in the case of a phase π-shift at the interface. We demonstrated that the temperature evolution of the conductance spectra can discriminate the physical origin of the conductance dips, either the formation of a localized magnetic moment or the presence of a weak proximized superconducting layer at the interface. According to the analysis, a localized magnetic moment could make a sign change of the superconducting order parameter energetically favorable. Finally, we used a discretized model to determine the necessary physical conditions under which the π-shift is realized: transparent interfaces can easily sustain a phase gradient as the effect of a weak interface magnetization, while for reduced transparencies a relative strong localized magnetization would be necessary.

Acknowledgments

We thank A. Braggio and F. Giazotto for helpful discussions. R.C. acknowledges the project FIRB-2012 Hybrid-NanoDev (Grant No. RBFR1236VV).

Author contribution statement

The authors state they have equally contributed to the paper.

References

1. Yu. G. Naidyuk and I. K. Yanson, *Point-contact spectroscopy*, (Springer, New York, 2005).
2. G. E. Blonder, M. Tinkham and T. M. Klapwijk, Phys. Rev. B **25**, 4515 (1982).
3. P. G. DeGennes, *Superconductivity Of Metals And Alloys*, (Westview Press, Boulder, 1999).
4. A. F. Andreev, Sov. Phys. JETP **51**, 111 (1980) [Zh. Eksp. Teor. Fis. **46**, 1823 (1964)].
5. R. J. Soulen, J. M. Byers, M. S. Osofsky, B. Nadgorny, T. Ambrose, S. F. Cheng, P. R. Broussard, C. T. Tanaka, J. Nowak, J. S. Moodera, A. Barry and J. M. D. Coey, Science **282**, 85 (1998).
6. S. K. Upadhyay, A. Palanisami, R. N. Louie, and R. A. Buhrman, Phys. Rev. Lett. **81**, 3247 (1998).
7. G. J. Strijkers, Y. Ji, F. Y. Yang and C. L. Chien, Phys. Rev. B **63**, 104510 (2001).
8. I. I. Mazin, A. A. Golubov, B. Nadgorny, J. Appl. Phys. **89**, 7576 (2001).
9. G. T. Woods, R. J. Soulen, Jr., I. Mazin, B. Nadgorny, M. S. Osofsky, J. Sanders, H. Srikanth, W. F. Egelhoff, and R. Datla, Phys. Rev. B **70**, 054416 (2004).
10. Y. Tanaka, A. A. Golubov and S. Kashiwaya, Phys. Rev. B **68**, 054513 (2003).
11. S. Kashiwaya, Y. Tanaka, M. Koyanagi and K. Kajimura, Phys. Rev. B **53**, 2667 (1996).
12. I. Žutić and O.T. Valls, Phys. Rev. B **61**, 1555 (2000).
13. N. L. Bobrov, S. I. Beloborodko, L. V. Tyutrina, I. K. Yanson, D. G. Naugle, and K. D. D. Rathnayaka, Phys. Rev. B **71**, 014512 (2005).
14. D. Daghero and R. S. Gonnelli, Supercond. Sci. Technol. **23**, 043001 (2010).
15. A. Pleceník, M. Grajcar, Š. Beňačka, P. Seidel, and A. Pfuch, Phys. Rev. B **49**, 10016 (1994).
16. Y. Miyoshi, Y. Bugoslavsky and L. F. Cohen, Phys. Rev. B **72**, 012502 (2005).
17. F. Giubileo, F. Romeo, R. Citro, A. Di Bartolomeo, C. Attanasio, C. Cirillo, A. Polcari, P. Romano, Physica C **503**, 158 (2014).
18. F. Giubileo, F. Romeo, R. Citro, A. Di Bartolomeo, C. Attanasio, C. Cirillo, A. Polcari, P. Romano, arXiv:1407.4906.
19. H. Srikanth and A. K. Raychaudhuri, Phys. Rev. B **46**, 14713 (1992).
20. Li Zhang-Zhi, Tao Hong-Jie, Xuan Yi, Ren Zhi-An, Che Guang-Can and Zhao Bai-Ru, Phys. Rev. B **66**, 064513 (2002).
21. P. Xiong, G. Xiao and R. B. Laibowitz, Phys. Rev. Lett. **71**, 1907 (1993).
22. G. Sheet, S. Mukhopadhyay and P. Raychaudhuri, Phys. Rev. B **69**, 134507 (2004).
23. M. Tinkham, *Introduction to superconductivity*, (McGraw-Hill, New York, 1996).
24. A. Barone and G. Paternò, *Physics and Applications of the Josephson effect*, (John Wiley & Sons, New York, 1982).
25. The presence of weak ferromagnetism in CuO has been reported, for instance, in C. B. Azzoni, A. Paleari and G. B. Parravicini, J. Phys.: Condens. Matter **4**, 1359 (1992).
26. J. A. Appelbaum, Phys. Rev. **154**, 633 (1967).
27. T. Kontos, M. Aprili, J. Lesueur and X. Grison, Phys. Rev. Lett. **86**, 304 (2001).

28. J. Bardeen, L. N. Cooper and J. R. Schrieffer, Phys. Rev. **108**, 1175 (1957).
29. The transparency of the interface is controlled by the on-site potential U. The interface opacity can be equivalently controlled coupling the magnetic impurity to the normal and superconducting side with different hopping values.
30. Notice that the spinorial particle-hole notation adopted in this work follows from the Bogoliubov field transformation $\psi_\sigma(x) = \sum_n [u_{n\sigma}(x)\gamma_n + v^*_{n\sigma}(x)\gamma^\dagger_n]$, with $x/a = i$. Using the Bogolons rapresentation the BCS Hamiltonian takes the form $H_{BCS} = \sum_n E_n \gamma^\dagger_n \gamma_n + E_g$.
31. The numerical results do not change taking $\lambda_i = \lambda \neq 0$ only in the S-region and in the proximized N-region whose extention is about $\xi \sim 10 \cdot a$.
32. F. S. Bergeret, A. Levy Yeyati, and A. Martín-Rodero, Phys. Rev. B **72**, 064524 (2005).